Journal of proteome research

pubs.acs.org/jpr

Article

# Metabolomic Profiling of the Aqueous Humor in Patients with Wet Age-Related Macular Degeneration Using UHPLC−MS/MS

Guoge Han,* Pinghui Wei, Meiqin He, He Teng, and Yanhua Chu

Cite This: https://dx.doi.org/10.1021/acs.jproteome.0c00036

Read Online

ACCESS | Metrics & More | Article Recommendations | Supporting Information

**ABSTRACT:** Assessing metabolomic alterations in age-related macular degeneration (AMD) can provide insights into its pathogenesis. We compared the metabolomic profiles of the aqueous humor between wet AMD patients ($n$ = 26) and age- and sex-matched patients undergoing cataract surgery without AMD as controls ($n$ = 20). A global untargeted metabolomics study was performed using ultra-high-performance liquid chromatography tandem mass spectrometry. Univariate analysis after the false discovery correction showed 18 significantly altered metabolites among the 291 metabolites measured. These differential metabolomic profiles pointed to three interconnected metabolic pathways: a compromised carnitine-associated mitochondrial oxidation pathway (carnitine, deoxycarnitine, N6-trimethyl-L-lysine), an altered carbohydrate metabolism pathway (*cis*-aconitic acid, itaconatic acid, and mesaconic acid), which plays a role in senescence and immunity, and an activated osmoprotection pathway (glycine betaine, creatine), which potentially contributes to the pathogenesis of the disease. These results suggested that metabolic dysfunction in AMD is mitochondrial-centered and may provide new insights into the pathophysiology of wet AMD and novel therapeutic strategies.

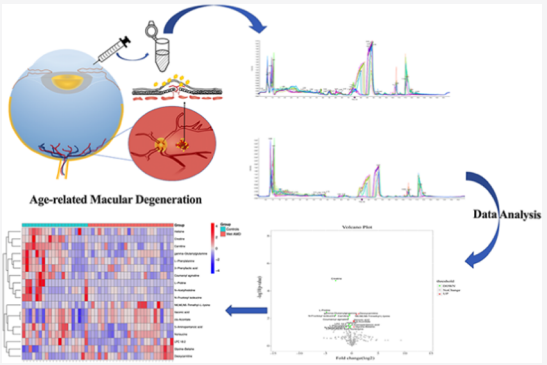


**KEYWORDS:** *metabolomic, aqueous humor (AH), age-related macular degeneration (AMD), mitochondrial*



## INTRODUCTION

Age-related macular degeneration (AMD), also known as macular degenerative disease, is becoming a leading cause of irreversible blindness in the aging population.[1] The worldwide prevalence of AMD has been reported to be 196 million thus far and is expected to increase to approximately 288 million by 2040.[2] AMD is classified into non-neovascular AMD and neovascular AMD (wet AMD), the latter being the major cause of severe vision loss in patients with macular degeneration.[3] The pathogenesis of the disease remains poorly understood; however, this is regarded to be a multifactorial disease caused by a genetic mitochondrial defect and metabolic dysfunction.[4,5] Evidence suggests that mitochondrial dysfunction could lead to elevated levels of reactive oxygen species (ROS), which may contribute to the progression of the disease.[6−8] Secondary to these changes, reprogramming of carbohydrate and lipid metabolism occurs in individuals with wet AMD.[9,10] Joyal et al.[11] suggested that the development of wet AMD may be driven by retinal metabolic dysregulation.

Metabolomics describes the analytical and informatic processes involved in characterizing and measuring multiple known and unknown metabolites in complex biological fluids, tissues, and cells. To date, metabolomic studies have focused on identifying metabolic changes at the plasma level in AMD patients.[12−14] However, the metabolome of the plasma is often influenced by potential confounding variables such as diet and lifestyle. In addition, previous studies suggested that local, rather than systemic, cytokine deregulation occurs in wet AMD.[15,16] The aqueous humor (AH) can partially reflect on the metabolic alterations that occur intraocularly. In fact, the AH metabolomic composition has previously been widely investigated in the anterior and posterior segments for other eye diseases, including glaucoma,[17] diabetic retinopathy (DR),[18,19] and myopia.[20,21] These studies indicated that the metabolic alteration from aqueous humor can reflect on the current phenotype of particular ocular diseases.[22]

Tandem mass spectrometry coupled with ultra-high-performance liquid chromatography (UHPLC−MS/MS) enables fast and sensitive analysis of small molecules in complex biological systems.[22−24] Therefore, in the current investigation, we performed UHPLC−MS/MS to identify the differential metabolites and metabolic pathways altered in wet AMD. Ultimately, we sought to provide further insight into the pathogenesis and determine the metabolic pathway that is altered in wet AMD. Thus, improving our understanding of

**Received:** January 23, 2020
**Published:** April 15, 2020

AMD-associated metabolic dysfunction may lead to the development of targeted therapies.

## EXPERIMENTAL SECTION

### Study Participants

This observational case−control study was designed to compare the metabolomic composition of wet AMD individuals with controls. Participants included in this study were 26 patients (26 eyes) diagnosed with wet AMD, who were first treated intravitreally with 0.5 mg of ranibizumab from April 2019 to June 2019. The wet AMD individuals were diagnosed according to spectral-domain optical coherence tomography (SD-OCT) and indocyanine green angiography (ICGA). The control group comprised 20 age- and sex-matched patients (20 eyes) undergoing cataract surgery without AMD. This study protocol was approved by the Tianjin Eye Hospital Ethics Committee, adhered to the tenets of the Declaration of Helsinki, and is registered online with the Chinese Clinical Trial Registry (ChiCTR1900022442). All participants recruited in the study provided written informed consent.

The exclusion criteria were as follows: the presence of any other vitreoretinal disease, active uveitis or ocular infection, primary or secondary glaucoma, corneal disease, significant media opacities, a mean spherical equivalent refractive error of −6 diopters or more, history of retinal surgery, history of any other ocular surgery or intraocular procedure (such as laser and intraocular injections), and diabetes mellitus, with or without concomitant DR. Participant age, sex, and health history were collected and analyzed.

### Sample Preparation

Approximately 100 $\mu$L of AH samples was collected with a fine needle from each patient at the beginning of the surgical intervention in the operating room. Undiluted samples were transferred into sterile containers and clarified by centrifugation in sterile tubes at 15 000$g$ for 5 min. Samples were immediately stored at −80 °C until UHPLC−MS analysis. During analysis, 100 $\mu$L of the sample was thoroughly mixed with 400 $\mu$L of cold methanol/acetonitrile (ACN) (v/v, 1:1) via vortexing. Then, the mixture was sonicated for 1 h in ice baths. The mixture was then incubated at −20 °C for 1 h and centrifuged at 4 °C for 20 min at a speed of 14 000$g$. The supernatants were then harvested and dried under vacuum. Additionally, to ensure data quality for metabolic profiling, quality control (QC) samples were prepared and analyzed using the same procedure as that for the experiment samples in each batch. Dried extracts were then dissolved in 50% ACN. Each sample was filtered through a disposable 0.22 $\mu$m cellulose acetate membrane and transferred into 2 mL HPLC vials and stored at −80 °C until analysis.

### UHPLC−MS/MS Analysis

Metabolic profiling of all samples was conducted based on a previous study.[25] Metabolites were analyzed using a UPLC system (UHPLC, 1290 Infinity LC, Agilent Technologies, Santa Clara, CA) coupled to a tandem mass spectrometer, TripleTOF 5600 Plus (AB Sciex, Framingham, MA).

For hydrophilic interaction liquid chromatography separation, samples were analyzed using an ACQUIY UPLC BEH Amide (2.1 mm × 100 mm, 1.7 $\mu$m) column (Waters, Ireland). The flow rate was 0.5 mL/min and the mobile phase contained A = 25 mM ammonium acetate and 25 mM ammonium hydroxide in water, and B = ACN. The gradient was programmed at 95% B for 0.5 min, then linearly reduced to 65% in 6.5 min, then further reduced to 40% in 2 min and maintained for 1 min, and then increased to 95% in 1.1 min with a 5 min re-equilibration period. Both positive-mode and negative-mode electrospray ionization (ESI) were applied for MS data acquisition. The ESI source conditions were set as follows: ion source gas 1 as 60, ion source gas 2 as 60, curtain gas as 30, source temperature as 600 °C, and ion spray voltage floating (ISVF) as 5500 V for the positive and −5500 V for the negative mode. During MS only acquisition, the instrument was set to acquire over the m/z range 60−1200 Da, and the accumulation time for TOF MS scanning was set at 0.15 s/spectra. During auto MS/MS acquisition, the instrument was set to acquire over the $m/z$ range 25−1200 Da, and the accumulation time for the product-ion scan was set at 0.03 s/spectra. The product-ion scan was acquired using information-dependent acquisition with the high-sensitivity mode selected. The collisional energy was fixed at 30 eV. Declustering potential was set at 60 V for both the positive and negative ion modes.

QC samples were prepared by pooling aliquots of all samples that were representative of the samples under analysis and used for data normalization. Blank samples (75% ACN in water) and QC samples were injected after every six samples during acquisition.

### Data Processing

The raw MS data were converted to MzXML files using ProteoWizard (version 3.06150) and processed using XCMS (version 3.2) for feature detection, retention time correction, and alignment. The combination of accurate mass (<25 ppm) and experimental MS/MS match against our in-house tandem MS spectral library and other public databases (NIST, and MassBank) was used for metabolite identification. In the extracted-ion features, metabolic peaks that were detected at less than 50% in all of the quality control (QC) samples were excluded. Only the variable ion peaks having more than 50% of the nonzero measurement values in at least one group were selected for statistical analysis.

SIMCAP software (version 14.0, Umetrics, Umeå, Sweden) was used for all multivariate data analyses and modeling. Data were mean-centered using Pareto scaling. Models were first built using principal component analysis (PCA) for the detection of sample grouping and outliers. Partial least-square discriminant analysis and orthogonal partial least-square discriminant analysis (OPLS-DA) were then applied to maximize the variation between the wet AMD and control group. All of the models evaluated were tested for overfitting using permutation test methods. The descriptive performance of the models was determined using $R^2X$ (cumulative) (perfect model: $R^2X$ (cum) = 1) and $R^2Y$ (cumulative) (perfect model: $R^2Y$ (cum) = 1) values, while their prediction performance was measured by Q2 (cumulative) (perfect model: $Q^2$ (cum) = 1) and a permutation test ($n$ = 200). The permuted model should not be able to predict classes: $R^2$ and $Q^2$ values at the $Y$-axis intercept must be lower than those of $Q^2$ and $R^2$ of the nonpermuted model. OPLS-DA allowed the determination of discriminating metabolites using the variable importance on projection (VIP).

The $P$-value was calculated by one-way analysis of variance (ANOVA) for multiple-groups analysis. Metabolites with VIP values >1.0 and $P$-values <0.05 were considered to be


https://dx.doi.org/10.1021/acs.jproteome.0c00036
J. Proteome Res. XXXX, XXX, XXX−XXX

statistically significant metabolites. Fold change was calculated as the logarithm of the average mass response (area) ratio between two arbitrary classes.

### KEGG Enrichment Analysis

KEGG pathway analysis using the KEGG database (https://www.kegg.jp/) was performed on the differential metabolite data to identify the biological pathways affected by wet AMD. To explore which metabolic pathways were altered in wet AMD patients, pathway analysis was performed by MetaboAnalyst 3.0. A $P$-value <0.05 and a count ≥3 were used as thresholds to identify the significantly altered metabolic pathways. KEGG enrichment analyses were carried out using a Fisher's exact test. False discovery rate (FDR) correction for multiple testing was also performed.

### Statistical Analysis

Statistical analysis was performed using SPSS software (GLM Univariate, version 21, IBM Corp.). An independent $t$-test was used to compare the mean of continuous variables between groups. Categorical variables were compared using the chi-squared test. All data were tested for Gaussian distribution. Pearson's correlation coefficients were computed to investigate linear relationships between variables. $P$-values <0.05 were considered statistically significant.

## RESULTS

### Clinical Characteristics of the Participants

The clinical characteristics of the participants are summarized in Table 1. The mean age and sex ratio between the wet AMD patients and the controls did not differ significantly ($P > 0.05$). There was no difference regarding the presence of hypertension, hyperlipidemia, cerebral infarction, and coronary heart disease between the two groups.

**Table 1. Characteristics of Subjects in Control and Wet AMD Groups**

| characteristic | controls ($n$ = 20) | wet AMD ($n$ = 26) | $P$-value |
|---|---|---|---|
| age (years) | 69.6 | 74.12 | 0.081 |
| male (%) | 65 | 53.85 | 0.446 |
| alcohol (%) | 5 | 11.5 | 0.435 |
| smokers (%) | 10 | 26.9 | 0.151 |
| hypertension (%) | 40 | 50 | 0.500 |
| hyperlipidemia (%) | 10 | 7.7 | 0.783 |
| cerebral infarction (%) | 5 | 23.1 | 0.09 |
| coronary heart disease (%) | 10 | 23.1 | 0.246 |

### AH Metabolic Profiles in Control and Wet AMD Subjects

Metabolic concentration data from the control and wet AMD groups were initially analyzed by PCA to assess the analytical run quality. As shown in Figure S1, partial overlaps between the two groups were observed. Typical total ion chromatograms of AH samples from the control and wet AMD subjects are shown in Figure 1. Supervised pattern recognition techniques were then applied using OPLS-DA to compare the metabolite profiles between the two groups. The results showed a clear separation between the wet AMD and control groups (Figure 2A). This was confirmed by cross-validation and permutation testing, which showed a cumulative $R^2Y$ of 0.993 and $Q^2$ of 0.736 (Figure 2B). A cluster of 200 permutated models was visualized using validation plots. The permutation test showed that all permuted $R^2$ and $Q^2$ values to the left were lower than the original point on the right and that the $Q^2$ regression line had a negative intercept, indicating that the models fit well.

### Metabolic Network Variation Based on the Altered Metabolites

In all, the concentrations of 18 metabolites were significantly different between the wet AMD and control groups (VIP > 1 and $P < 0.05$) among the 291 metabolites measured. All of these 291 detected metabolites are shown in Table S1. Among them, 5 metabolites showed significantly higher concentrations, while 13 showed lower concentrations in the wet AMD group compared to the controls. Fold changes (FC) were used to show the differences between the two groups (Table 2). All metabolites were confirmed by the library database, since no authentic standards were commercially available. Of these metabolites, L-proline exhibited the highest-fold decrease (FC = 0.035), followed by $N$-fructosyl isoleucine (FC = 0.113) and creatine (FC = 0.116). As shown in Figure 3, other metabolites that were decreased in the wet AMD group included L-carnitine, $N$-acetylhistidine, and lysophosphatidylcholine (LP) 18:2. The metabolites that were significantly increased included itaconic acid, *cis*-aconitate, deoxycarnitine, N6-trimethyl-L-lysine (TML), and glycine betaine (GB).

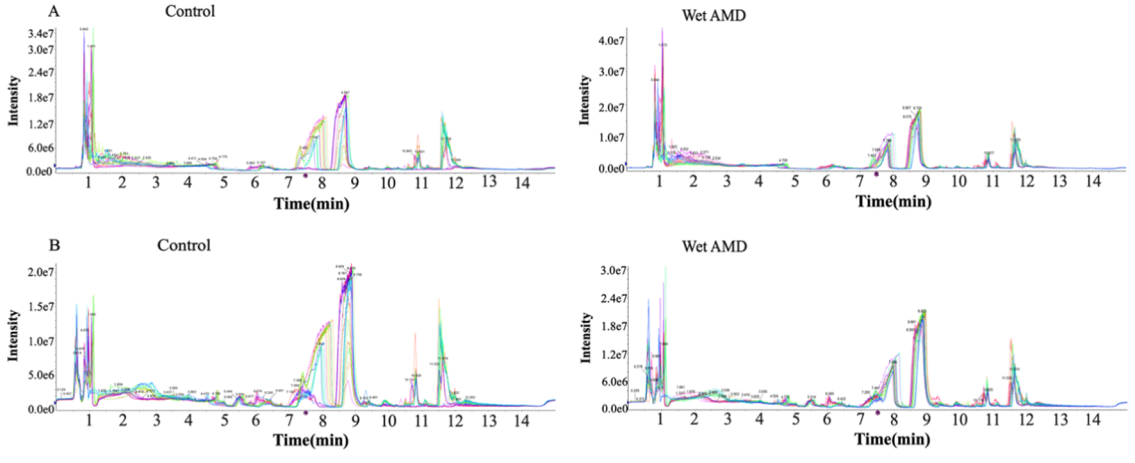


**Figure 1.** Representative aqueous humor metabolic profiling from control and wet AMD subjects in positive (A) and negative (B) ESI modes.


https://dx.doi.org/10.1021/acs.jproteome.0c00036
J. Proteome Res. XXXX, XXX, XXX−XXX

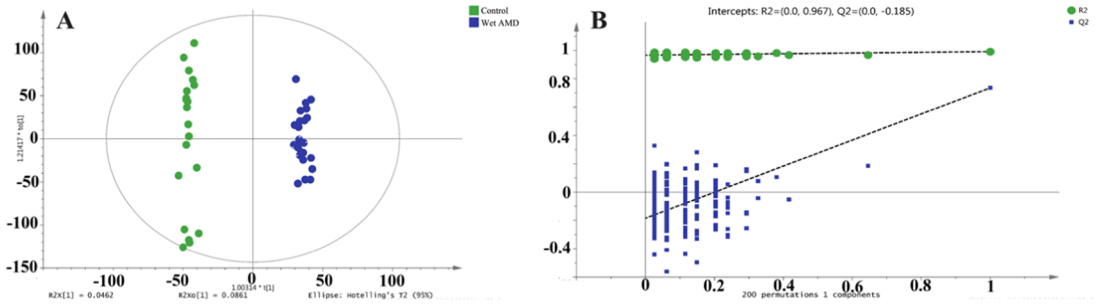


**Figure 2.** Significant disturbed metabolite analysis. (A) Orthogonal projection to latent structure discriminant analysis (OPLS-DA) between the control and wet AMD groups. (B) Permutation test of the OPLS-DA model.

**Table 2. List of Metabolites Significantly Differentiating Aqueous Humor Metabolic Profiles of the Patients with Wet AMD and Controls by UHPLC−MS/MS Analysis**

| metabolite | *m/z* | *RT* (s) | VIP | FC | *P*-value |
|---|---|---|---|---|---|
| deoxycarnitine | 146.1175 | 8.4 | 1.8719 | 2.40204987 | 0.00455042 |
| N6,N6,N6-trimethyl-L-lysine | 189.1604 | 12.5 | 1.84775 | 1.77961665 | 0.00533871 |
| glycine betaine | 118.0863 | 11.05 | 1.56267 | 1.3029007 | 0.0412461 |
| itaconic acid | 129.0206 | 11.37 | 1.70405 | 1.28297886 | 0.01505469 |
| *cis*-aconitate | 173.0092 | 11.37 | 1.67156 | 1.27602732 | 0.01727889 |
| 5-aminopentanoic acid | 116.0727 | 7.41 | 1.43728 | 0.85177776 | 0.03325281 |
| norleucine | 132.1012 | 6.44 | 1.28093 | 0.80719541 | 0.04740267 |
| L-phenylalanine | 164.0727 | 6.23 | 1.48879 | 0.7636036 | 0.03880729 |
| carnitine | 162.1125 | 8.93 | 1.86561 | 0.71709546 | 0.00627448 |
| γ-glutamylglutamine | 276.119 | 11.18 | 1.88249 | 0.69451232 | 0.00520636 |
| hetisine | 374.1998 | 0.88 | 1.53244 | 0.67999269 | 0.0263322 |
| 3-phenyllactic acid | 165.0565 | 1.1 | 1.44928 | 0.6719715 | 0.04626954 |
| LPC 18:2 | 520.3405 | 3.99 | 1.42621 | 0.64317951 | 0.02862951 |
| coumaroyl agmatine | 277.1658 | 6.15 | 1.72538 | 0.60026033 | 0.00986845 |
| *N*-acetylhistidine | 198.0853 | 7.99 | 1.45553 | 0.45796294 | 0.0417775 |
| creatine | 132.0768 | 8.78 | 2.73223 | 0.1167791 | $1.7953 \times 10^{-5}$ |
| *N*-fructosyl isoleucine | 294.1551 | 7.92 | 1.91879 | 0.11336595 | 0.00580632 |
| L-proline | 116.071 | 7.83 | 2.02077 | 0.03527375 | 0.00348076 |

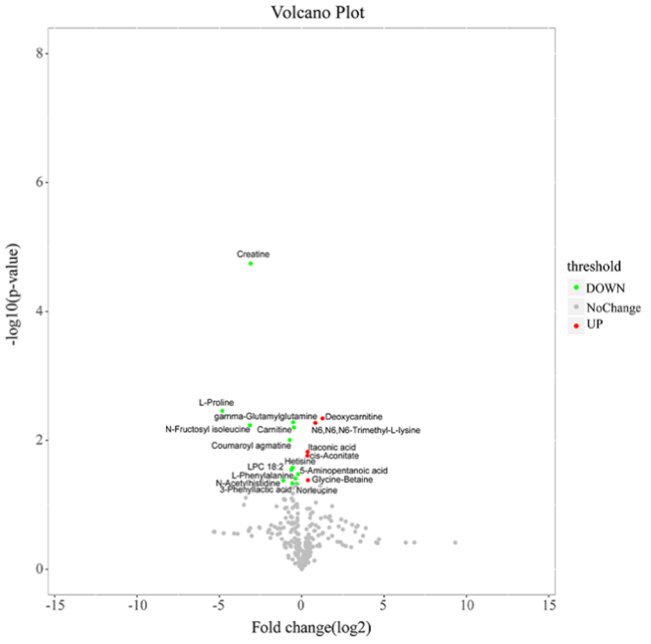


**Figure 3.** Volcano plot representing the relationship between fold change and significance of metabolic features forwarded for statistical analysis.

Additionally, heatmap plots were created to better visualize the differences in metabolite concentrations between the two groups and to classify the upregulated and downregulated metabolites (Figure S2).

## Metabolic Pathway Analysis

Upon identifying the metabolites that were significantly altered between the wet AMD and control groups, a KEGG pathway analysis was performed to identify the biological pathways affected by wet AMD. Ten pathways were found to be altered in wet AMD patients; the pathways that were most significantly enriched were involved in arginine and proline metabolism (*P*-value = $4.9 \times 10^{-6}$), lysine degradation (*P*-value = $4.37 \times 10^{-5}$), and ABC transportion (*P*-value = $1.59 \times 10^{-5}$) (Figure 4).

## Metabolite−Metabolite Correlation Analysis of the AH

A Pearson pair-wise correlation analysis was performed between metabolites to investigate the regulatory metabolic network in AH in individuals with wet AMD (Figure S3). Of note, *cis*-aconitate had the greatest significant positive correlation with itaconic acid, while both *cis*-aconitate and itaconic acid negatively correlated with L-proline. Additionally, there was a strong correlation between carnitine and creatine.


https://dx.doi.org/10.1021/acs.jproteome.0c00036
J. Proteome Res. XXXX, XXX, XXX−XXX

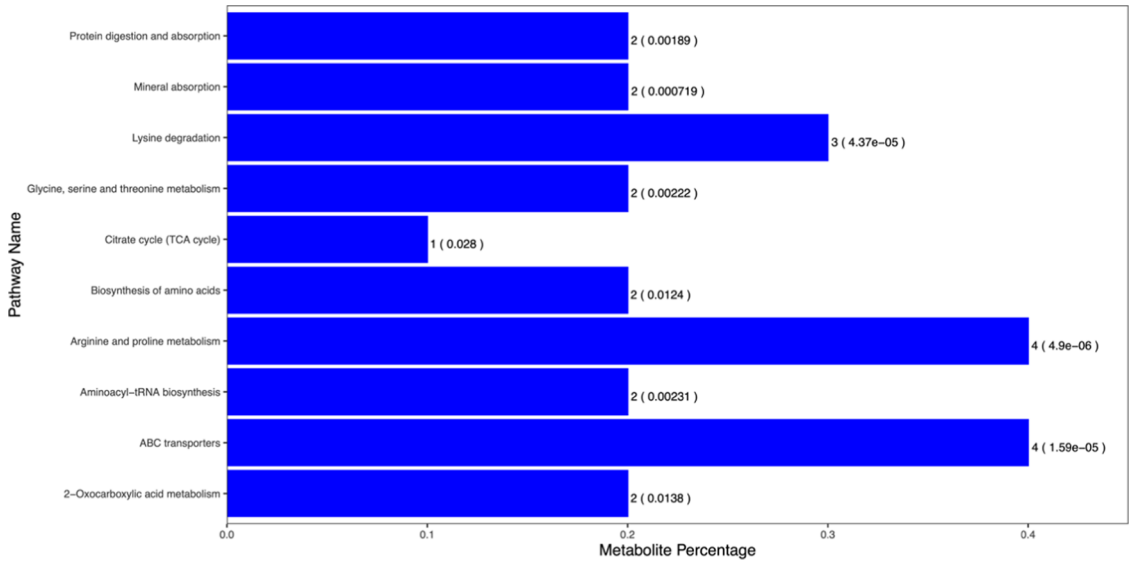


**Figure 4.** Metabolic pathway analysis was performed with MetaboAnalyst 3.0. The calculated *P*-value was established based on the pathway enrichment analysis, while the pathway impact value was based on the pathway topology analysis; the count is the matched number from the user uploaded data.

## DISCUSSION

The current study found 18 significantly altered metabolites in patients with wet AMD after FDR correction. These results point to a comprehensive metabolic signature in wet AMD by combining mitochondrial dysfunction-associated altered amino acid metabolism (L-proline), energetic substrates (carnitine, deoxycarnitine, TML), and compromised carbohydrate metabolism (*cis*-aconitic acid and itaconate acid). Among these metabolites, *cis*-aconitic acid and itaconate acid are known to be linked with age-related oxidative stress[26,27] and innate immunity.[28] Other metabolites such as glycine betaine and creatine are involved in osmoprotection,[29] highlighting their importance in the pathogenesis of AMD.

The decreased concentration of L-proline has not been previously investigated in the AH of AMD patients. Proline, synthesized from glutamate/glutamine, serves as an alternative source of energy during stress or hypoxia and controls mitochondrial function for maintaining redox balance.[30] Previous global metabolomics research has found higher levels of L-proline in early AMD and lower levels during intermediate or late AMD, which is equivalent to the wet AMD in our cohort.[13] In line with this result, we also found that the concentration of L-proline was significantly reduced in the AH of wet AMD (FC = 0.035, $P$ = 0.003). The decrease in L-proline concentration may play an important role in the pathogenesis of AMD. Interestingly, recent papers have suggested that proline is a preferable nutrient substrate in human retinal pigment epithelial (RPE) cells, and that exporting proline-derived mitochondrial products for use in the outer retina serves in protecting against oxidative damage.[31]

Carnitine plays an essential function in shuttling long-chain fatty acids into the mitochondrial matrix for $\beta$-oxidation and acts as an antioxidant.[32] Emerging evidence suggests that disturbance of the carnitine pathway leads to impaired mitochondrial function, which ultimately results in perturbation of cellular neuroprotective and antioxidant properties, accompanied by increasing mitochondrial dysfunction and cell death.[33,34] The precursor for carnitine biosynthesis is obtained mainly from lysine degradation. Carnitine is synthesized from its substrate 6-*N*-trimethyllysine (TML), which gets hydroxylated from deoxycarnitine by $\gamma$-butyrobetaine dioxygenase to generate carnitine.[35] Interestingly, in this study, we found that the concentrations of TML and deoxycarnitine were both significantly increased, accompanied by significantly decreased L-carnitine levels. An increase in TML and deoxycarnitine concentration is associated with amino acid degradation, which supports the concept that disruption of protein and amino acid homeostasis may be one of the underlying mechanisms leading to AMD.[36] In line with this suggestion, a pioneer investigation by Laíns et al. on the metabolic profile of plasma in AMD patients also detected lower lysine levels compared with controls.[13]

The metabolic signature of free carnitine and acylcarnitine has not been previously investigated in the AH of AMD patients, although previous plasma studies have found that the carnitine shuttling pathway may be involved in the pathophysiology of wet AMD.[14,37] In addition, an increased plasma concentration of long-chain acylcarnitine has been reported in different AMD cohorts. The decreased level of free carnitine found in the current study may indicate the upregulation of esterification to generate acylcarnitine derivatives. We also found higher acylcarnitine and butyryl carnitine levels in AMD patients than in controls, although the difference was not significant. This could possibly be owing to the higher level of free carnitine present in the AH from AMD patients than in the choroid-retina and plasma, leading to lower levels of its esterified form, such as acylcarnitine.[38,39] In addition, the relatively small number of participants or the single-center nature of this study may also contribute to the lack of significant difference in acylcarnitine levels observed. Previous research has demonstrated that long-chain acetyl-L-carnitine levels were increased in patients with neovascular AMD[37] and that L-carnitine has the potential to protect the retina from ischemia-reperfusion injury.[40] Together, this suggests that fatty acid metabolism, especially alteration of the carnitine pathway, may be involved in the pathophysiology of wet AMD.


https://dx.doi.org/10.1021/acs.jproteome.0c00036
J. Proteome Res. XXXX, XXX, XXX−XXX

*cis*-Aconitic acid (CAA), an intermediate substrate during the conversion of citrate to isocitrate in the tricarboxylic acid cycle (TCA), is synthesized by mitochondrial aconitase (*Acon*) in humans.[41] In a Drosophila model (*Acon*-knockdown, Acon), high levels of *cis*-aconitate, induced by low *m*-aconitase activity, led to increased cell death in the brain via the impairment of glycolysis and the TCA cycle and depletion of ATP levels.[42] Interestingly, a point mutation in the *m*-aconitase encoding gene was found to cause retinal degeneration.[43] Indeed, impaired aconitase activity, which leads to accumulation of CAA, was also specifically targeted/affected by oxidative damage during aging.[26] In a genetic polymorphism AMD population study, iron-regulatory protein 1 (IRP1), known as the cytosolic aconitase, was shown to be associated with an increased risk of developing wet AMD.[27] Thus, due to IRP1 or aconitase production, CAA possibly links metabolism with the aging processes and oxidative stress by altering oxidative phosphorylation and fatty acid oxidation. In line with these suggestions, the significant increase in the concentration of CAA, as first reported in this study, might manifest its essential role in the pathogenesis of this disease.

Itaconic acid, generated from *cis*-aconitate via decarboxylase (immunoresponsive gene 1, *IRG1*), is known to be an immunoregulatory metabolite, which links innate immunity with TCA cycle remodeling.[28,44] A significant increase in itaconic acid concentration caused by inflammatory macrophage activation was found to modulate succinate concentration, subsequently regulating the interleukin-1$\beta$-hypoxia-inducible factor-1$\alpha$ axis, accompanied by cytokine production.[45] In fact, activation of senescent macrophages by interleukin plays an essential role during vascular proliferation in the mice choroidal neovascularization (CNV) models.[46] However, no published paper has focused on itaconate's immunoregulatory role and metabolism reprogramming properties from AMD studies. Given that itaconic acid AH level was highly increased in AMD patients, future work should be performed on the possible underlying mechanism by which itaconic acid acts as a modulator by linking innate immunity, glucose metabolism, and neovascular proliferation.

Glycine betaine (GB) was previously regarded as an osmoprotector and is now widely accepted to play a regulatory role in carbohydrate metabolism, oxidative stress, and fatty oxidation.[29] In an epidemiological AMD study, a relatively higher salt intake led to increased extracellular osmolarity. This is a risk factor for AMD and has detrimental effects on the RPE and vascular tissue in vitro.[47] It was suggested that hypertonic stress stimulates inflammatory mediators and vascular endothelial growth factor (VEGF) production in RPE cells.[48] Thus, in terms of its role as an osmoprotector, we speculated that the increased GB concentration in the AMD group protects the impaired cells or dysfunctional enzymes from environmental stress and dietary habits, since the cohort was from a high salt-intake area in North China. Apart from regulating hypertonicity, GB has also been shown to inhibit retinal neovascularization in oxygen-induced retinopathy models and streptozotocin-induced hyperglycemic rat models.[49,50] Based on the previous suggestion, the significant increase in the concentration of CAA, as first reported in this study, may indicate its potential role in the pathogenesis of wet AMD.

Upon comparison of our results with previous studies, some of the metabolites altered in the AH of patients with AMD were not found to be altered in the plasma. This suggested that AMD might also affect the permeability of the BAB (blood aqueous barrier).[13,14,37,51] Although AMD is regarded as a disease of the posterior segment and is associated with CNV and cytokine or complement protein infiltration via the compromised BRB (blood retina barrier), the BAB and BRB share similar structural properties and are believed to work cooperatively in response to stress.[52−54] Therefore, it is plausible that the alteration of certain metabolites in the AH might partially reflect on the metabolic profiles in the affected retina caused by the leakage from the BRB. In addition, Agrawal et al. evaluated the cytokine profiles in both the AH and blood samples of CNV-AMD patients.[16] They found significant differences in cytokine levels between the AH and plasma. Thus, they suggested that local rather than systemic deregulation of cytokine production occurs in CNV-AMD. Furthermore, this result is supported by the study that compared the cytokine profile in the AH and serum between AMD patients and healthy controls.[15] However, this suggestion does not support the concept that since the anterior segments are topographically closer to the AH the ciliary body might also affect the metabolic signature of the AH more than the retina. Indeed, Riley et al. performed an in vivo experiment to elucidate the nature and extent of lactic acid shuttling between the AH and their surroundings.[55] They concluded that, in addition to the cornea and lens, both the ciliary body and the retina were a significant source of lactate to the AH. This paper, although published four decades ago, made ground for using AH as a source for analyzing metabolism in the eye by comparing the AH with plasma and vitreous humor. Unfortunately, no further research has investigated other metabolites or the retinal disease model using AH as a source. At this stage, we concluded that the metabolic dynamics of the AH is intermediary, as it is affected by both the retina and ciliary body. We are undertaking similar animal studies with the purpose of elucidating the differences in metabolic profiles between the AH and vitreous humor, as well as the retina in various retinal disease models, to provide more precise and solid evidence in the future.

This study has a few limitations, the first being the small number of participants included in this study. We found that, with the sample size used, the mean and standard deviation of associated metabolites gave a statistical power of >0.8. After searching the related literature, we found that 20 samples are generally sufficient to evaluate the sample size in a rigorous manner.[56] Controlled clinical studies where the subjects are carefully matched can be carried out with as few as 10−20 patients.[57] Hence, we believe that although the number of recruited patients was relatively small, it was enough to detect the difference between the two groups. Second, this cohort did not include other AMD subtypes such as dry or early-stage AMD. This is because only late-stage AMD participants were treated with intravitreal VEGF therapy; thus, only these patients were available for AH specimen collection. Additionally, this cohort encompassed only Northern Chinese patients, whose dietary habits and environmental factors may affect the results. Another concern was that the extent of AH metabolism reflects on the compromised retinal metabolism. We fully understood that the vitreous humor and even macular tissue specimen from AMD patients would be ideal, due to being closer to the CNV. However, it is more invasive to obtain vitreous samples and may not be ethically justified in our research. Lastly, the metabolic profile of the AH is dynamic, and can be affected by a number of factors (such as specimen


https://dx.doi.org/10.1021/acs.jproteome.0c00036
J. Proteome Res. XXXX, XXX, XXX−XXX

preservation approach and method of measurement). Further experiments or other cohorts are needed to validate our conclusion, assess the significantly altered metabolites quantitatively, and explore the diversity of the targeted metabolic pathways.

## CONCLUSIONS

This is the first study to assess the metabolomic profiles of AH in wet AMD patients. We found four major features: (1) altered amino acid metabolism, including reduced levels of L-proline and increased concentration of TML and deoxycarnitine via protein−lysine degradation, (2) significant decrease in free carnitine levels and increase in certain acylcarnitines, suggesting a role of the carnitine shuttling pathway, (3) metabolic remodeling of the TCA cycle and carbohydrate metabolism (e.g., CAA and itaconatic acid), and (4) increased concentration of GB involved in the osmoprotection pathway. These results suggest that mitochondrial dysfunction as well as altered carbohydrate, amino acid, and fatty acid metabolism potentially contributes to the pathogenesis of wet AMD. Further investigation will be required to confirm the above results and investigate further the metabolic pathways involved in wet AMD, potentially leading to a more comprehensive understanding of the pathophysiology of this disease.

## ASSOCIATED CONTENT

### Supporting Information

The Supporting Information is available free of charge at https://pubs.acs.org/doi/10.1021/acs.jproteome.0c00036.

Score plots of the principal component analysis (PCA) from the wet AMD and control groups. t[1] = first principal component; t[2] = second principal component (Figure S1); heatmap representation of the 18 metabolites across the 35 samples (Figure S2); Spearman correlation analysis of all of the significantly altered metabolites (VIP > 1 and $p < 0.05$) (Figure S3) (PDF)

Excel document of all detected metabolites (Table S1) (XLSX)

## AUTHOR INFORMATION


### Corresponding Author

**Guoge Han** − *Tianjin Eye Hospital, Tianjin Key Laboratory of Ophthalmology and Visual Science, Tianjin 300020, P. R. China;* orcid.org/0000-0003-0079-3023; Email: dovehanguoge@hotmail.com

### Authors

**Pinghui Wei** − *Tianjin Eye Hospital, Tianjin Key Laboratory of Ophthalmology and Visual Science, Tianjin 300020, P. R. China*

**Meiqin He** − *Tianjin Eye Hospital, Tianjin Key Laboratory of Ophthalmology and Visual Science, Tianjin 300020, P. R. China*

**He Teng** − *Eye Institute and School of Optometry and Ophthalmology, Tianjin Medical University Eye Hospital, Tianjin 300384, P. R. China*

**Yanhua Chu** − *Tianjin Eye Hospital, Tianjin Key Laboratory of Ophthalmology and Visual Science, Tianjin 300020, P. R. China*

Complete contact information is available at: https://pubs.acs.org/10.1021/acs.jproteome.0c00036


### Author Contributions

G.H., P.W., and M.H. conceived the experimental plan, all authors performed the experiments, and G.H. and P.W. analyzed the data and wrote the manuscript. All authors have given approval to the final version of the manuscript.


### Funding

This work was supported by a grant from the National Natural Science Foundation of China (81700849) and Natural Science Foundation of Tianjin City (18JCQNJC10600).


### Notes

The authors declare no competing financial interest.

## ABBREVIATIONS USED

ACN, acetonitrile; AH, aqueous humor; AMD, age-related macular degeneration; ANOVA, analysis of variance; CAA, *cis*-aconitic acid; CNV, choroidal neovascularization; DR, diabetic retinopathy; ESI, electrospray ionization; FC, fold change; FDR, false discovery rate; GB, glycine betaine; IRP-1, iron-regulatory protein 1; OPLS-DA, orthogonal partial least-square discriminant analysis; PCA, principal component analysis; QC, quality control; RPE, retinal pigment epithelial; TCA, tricarboxylic acid cycle; TML, 6-*N*-trimethyllysine; UHPLC−MS/MS, ultra-high-performance liquid chromatography; VEGF, vascular endothelial growth factor; VIP, variable importance on projection

## REFERENCES


(1) Jonas, J. B.; Cheung, C. M. G.; Panda-Jonas, S. Updates on the Epidemiology of Age-Related Macular Degeneration. *Asia-Pac. J. Ophthalmol.* **2017**, *6*, 493−497.

(2) Wong, W. L.; Su, X.; Li, X.; Cheung, C. M.; Klein, R.; Cheng, C. Y.; Wong, T. Y. Global prevalence of age-related macular degeneration and disease burden projection for 2020 and 2040: a systematic review and meta-analysis. *Lancet Global Health* **2014**, *2*, e106−e116.

(3) Kaur, C.; Foulds, W. S.; Ling, E. A. Hypoxia-ischemia and retinal ganglion cell damage. *Clin. Ophthalmol.* **2008**, *2*, 879−89.

(4) van Lookeren Campagne, M.; LeCouter, J.; Yaspan, B. L.; Ye, W. Mechanisms of age-related macular degeneration and therapeutic opportunities. *J. Pathol.* **2014**, *232*, 151−64.

(5) Al-Zamil, W. M.; Yassin, S. A. Recent developments in age-related macular degeneration: a review. *Clin. Interventions Aging* **2017**, *12*, 1313−1330.

(6) Brown, E. E.; Lewin, A. S.; Ash, J. D. Mitochondria: Potential Targets for Protection in Age-Related Macular Degeneration. *Adv. Exp. Med. Biol.* **2018**, *1074*, 11−17.

(7) Nashine, S.; Nesburn, A. B.; Kuppermann, B. D.; Kenney, M. C. Age-related macular degeneration (AMD) mitochondria modulate epigenetic mechanisms in retinal pigment epithelial cells. *Exp. Eye Res.* **2019**, *189*, No. 107701.

(8) Nashine, S.; Cohen, P.; Chwa, M.; Lu, S.; Nesburn, A. B.; Kuppermann, B. D.; Kenney, M. C. Humanin G (HNG) protects age-related macular degeneration (AMD) transmitochondrial ARPE-19 cybrids from mitochondrial and cellular damage. *Cell Death Dis.* **2017**, *8*, No. e2951.

(9) Brown, E. E.; DeWeerd, A. J.; Ildefonso, C. J.; Lewin, A. S.; Ash, J. D. Mitochondrial oxidative stress in the retinal pigment epithelium (RPE) led to metabolic dysfunction in both the RPE and retinal photoreceptors. *Redox Biol.* **2019**, *24*, No. 101201.

(10) Kersten, E.; Paun, C. C.; Schellevis, R. L.; Hoyng, C. B.; Delcourt, C.; Lengyel, I.; Peto, T.; Ueffing, M.; Klaver, C. C. W.; Dammeier, S.; den Hollander, A. I.; de Jong, E. K. Systemic and ocular fluid compounds as potential biomarkers in age-related macular degeneration. *Surv. Ophthalmol.* **2018**, *63*, 9−39.




https://dx.doi.org/10.1021/acs.jproteome.0c00036
J. Proteome Res. XXXX, XXX, XXX−XXX

(11) Joyal, J. S.; Sun, Y.; Gantner, M. L.; Shao, Z.; Evans, L. P.; Saba, N.; Fredrick, T.; Burnim, S.; Kim, J. S.; Patel, G.; Juan, A. M.; Hurst, C. G.; Hatton, C. J.; Cui, Z.; Pierce, K. A.; Bherer, P.; Aguilar, E.; Powner, M. B.; Vevis, K.; Boisvert, M.; Fu, Z.; Levy, E.; Fruttiger, M.; Packard, A.; Rezende, F. A.; Maranda, B.; Sapieha, P.; Chen, J.; Friedlander, M.; Clish, C. B.; Smith, L. E. Retinal lipid and glucose metabolism dictates angiogenesis through the lipid sensor Ffar1. *Nat. Med.* **2016**, *22*, 439−45.

(12) Osborn, M. P.; Park, Y.; Parks, M. B.; Burgess, L. G.; Uppal, K.; Lee, K.; Jones, D. P.; Brantley, M. A., Jr. Metabolome-wide association study of neovascular age-related macular degeneration. *PLoS one* **2013**, *8*, No. e72737.

(13) Laíns, I.; Duarte, D.; Barros, A. S.; Martins, A. S.; Gil, J.; Miller, J. B.; Marques, M.; Mesquita, T.; Kim, I. K.; Cachulo, M. D. L.; Vavvas, D.; Carreira, I. M.; Murta, J. N.; Silva, R.; Miller, J. W.; Husain, D.; Gil, A. M. Human plasma metabolomics in age-related macular degeneration (AMD) using nuclear magnetic resonance spectroscopy. *PLoS one* **2017**, *12*, No. e0177749.

(14) Laíns, I.; Kelly, R. S.; Miller, J. B.; Silva, R.; Vavvas, D. G.; Kim, I. K.; Murta, J. N.; Lasky-Su, J.; Miller, J. W.; Husain, D. Human Plasma Metabolomics Study across All Stages of Age-Related Macular Degeneration Identifies Potential Lipid Biomarkers. *Ophthalmology* **2018**, *125*, 245−254.

(15) Spindler, J.; Zandi, S.; Pfister, I. B.; Gerhardt, C.; Garweg, J. G. Cytokine profiles in the aqueous humor and serum of patients with dry and treated wet age-related macular degeneration. *PLoS One* **2018**, *13*, No. e0203337.

(16) Agrawal, R.; Balne, P. K.; Wei, X.; Bijin, V. A.; Lee, B.; Ghosh, A.; Narayanan, R.; Agrawal, M.; Connolly, J. Cytokine Profiling in Patients With Exudative Age-Related Macular Degeneration and Polypoidal Choroidal Vasculopathy. *Invest. Ophthalmol. Visual Sci.* **2019**, *60*, 376−382.

(17) Mayordomo-Febrer, A.; Lopez-Murcia, M.; Morales-Tatay, J. M.; Monleon-Salvado, D.; Pinazo-Duran, M. D. Metabolomics of the aqueous humor in the rat glaucoma model induced by a series of intracamerular sodium hyaluronate injection. *Exp. Eye Res.* **2015**, *131*, 84−92.

(18) Jin, H.; Zhu, B.; Liu, X.; Jin, J.; Zou, H. Metabolic characterization of diabetic retinopathy: An (1)H-NMR-based metabolomic approach using human aqueous humor. *J. Pharm. Biomed. Anal.* **2019**, *174*, 414−421.

(19) Wang, H.; Fang, J.; Chen, F.; Sun, Q.; Xu, X.; Lin, S. H.; Liu, K. Metabolomic profile of diabetic retinopathy: a GC-TOFMS-based approach using vitreous and aqueous humor. *Acta Diabetol.* **2020**, *57*, 41−51.

(20) Barbas-Bernardos, C.; Armitage, E. G.; Garcia, A.; Merida, S.; Navea, A.; Bosch-Morell, F.; Barbas, C. Looking into aqueous humor through metabolomics spectacles - exploring its metabolic characteristics in relation to myopia. *J. Pharm. Biomed. Anal.* **2016**, *127*, 18−25.

(21) Ji, Y.; Rao, J.; Rong, X.; Lou, S.; Zheng, Z.; Lu, Y. Metabolic characterization of human aqueous humor in relation to high myopia. *Exp. Eye Res.* **2017**, *159*, 147−155.

(22) Wei, P.; He, M.; Teng, H.; Han, G. Quantitative analysis of metabolites in glucose metabolism in the aqueous humor of patients with central retinal vein occlusion. *Exp. Eye Res.* **2020**, *191*, No. 107919.

(23) Santos-Fandila, A.; Zafra-Gomez, A.; Barranco, A.; Navalon, A.; Rueda, R.; Ramirez, M. Quantitative determination of neurotransmitters, metabolites and derivates in microdialysates by UHPLC-tandem mass spectrometry. *Talanta* **2013**, *114*, 79−89.

(24) Tang, Z.; Cao, T.; Lin, S.; Fu, L.; Li, S.; Guan, X. Y.; Cai, Z. Characterization of oncogene-induced metabolic alterations in hepatic cells by using ultrahigh performance liquid chromatography-tandem mass spectrometry. *Talanta* **2016**, *152*, 119−26.

(25) Liang, L.; Liu, G.; Yu, G.; Zhang, F.; Linhardt, R. J.; Li, Q. Urinary metabolomics analysis reveals the anti-diabetic effect of stachyose in high-fat diet/streptozotocin-induced type 2 diabetic rats. *Carbohydr. Polym.* **2020**, *229*, No. 115534.

(26) Yan, L. J.; Levine, R. L.; Sohal, R. S. Oxidative damage during aging targets mitochondrial aconitase. *Proc. Natl. Acad. Sci. U.S.A.* **1997**, *94*, 11168−11172.

(27) Synowiec, E.; Pogorzelska, M.; Blasiak, J.; Szaflik, J.; Szaflik, J. P. Genetic polymorphism of the iron-regulatory protein-1 and -2 genes in age-related macular degeneration. *Mol. Biol. Rep.* **2012**, *39*, 7077−7087.

(28) Bambouskova, M.; Gorvel, L.; Lampropoulou, V.; Sergushichev, A.; Loginicheva, E.; Johnson, K.; Korenfeld, D.; Mathyer, M. E.; Kim, H.; Huang, L. H.; Duncan, D.; Bregman, H.; Keskin, A.; Santeford, A.; Apte, R. S.; Sehgal, R.; Johnson, B.; Amarasinghe, G. K.; Soares, M. P.; Satoh, T.; Akira, S.; Hai, T.; de Guzman Strong, C.; Auclair, K.; Roddy, T. P.; Biller, S. A.; Jovanovic, M.; Klechevsky, E.; Stewart, K. M.; Randolph, G. J.; Artyomov, M. N. Electrophilic properties of itaconate and derivatives regulate the IkappaBzeta-ATF3 inflammatory axis. *Nature* **2018**, *556*, 501−504.

(29) Figueroa-Soto, C. G.; Valenzuela-Soto, E. M. Glycine betaine rather than acting only as an osmolyte also plays a role as regulator in cellular metabolism. *Biochimie* **2018**, *147*, 89−97.

(30) Szabados, L.; Savoure, A. Proline: a multifunctional amino acid. *Trends Plant Sci.* **2010**, *15*, 89−97.

(31) Yam, M.; Engel, A. L.; Wang, Y.; Zhu, S.; Hauer, A.; Zhang, R.; Lohner, D.; Huang, J.; Dinterman, M.; Zhao, C.; Chao, J. R.; Du, J. Proline mediates metabolic communication between retinal pigment epithelial cells and the retina. *J. Biol. Chem.* **2019**, *294*, 10278−10289.

(32) Almannai, M.; Alfadhel, M.; El-Hattab, A. W. Carnitine Inborn Errors of Metabolism. *Molecules* **2019**, *24*, No. 3251.

(33) Calandrella, N.; De Seta, C.; Scarsella, G.; Risuleo, G. Carnitine reduces the lipoperoxidative damage of the membrane and apoptosis after induction of cell stress in experimental glaucoma. *Cell Death Dis.* **2010**, *1*, No. e62.

(34) Buisset, A.; Gohier, P.; Leruez, S.; Muller, J.; Amati-Bonneau, P.; Lenaers, G.; Bonneau, D.; Simard, G.; Procaccio, V.; Annweiler, C.; Milea, D.; Reynier, P.; Chao de la Barca, J. M. Metabolomic Profiling of Aqueous Humor in Glaucoma Points to Taurine and Spermine Deficiency: Findings from the Eye-D Study. *J. Proteome Res.* **2019**, *18*, 1307−1315.

(35) Strijbis, K.; Vaz, F. M.; Distel, B. Enzymology of the carnitine biosynthesis pathway. *IUBMB life* **2010**, *62*, 357−62.

(36) Ferrington, D. A.; Sinha, D.; Kaarniranta, K. Defects in retinal pigment epithelial cell proteolysis and the pathology associated with age-related macular degeneration. *Prog. Retinal Eye Res.* **2016**, *51*, 69−89.

(37) Mitchell, S. L.; Uppal, K.; Williamson, S. M.; Liu, K.; Burgess, L. G.; Tran, V.; Umfress, A. C.; Jarrell, K. L.; Cooke Bailey, J. N.; Agarwal, A.; Pericak-Vance, M.; Haines, J. L.; Scott, W. K.; Jones, D. P.; Brantley, M. A., Jr. The Carnitine Shuttle Pathway is Altered in Patients With Neovascular Age-Related Macular Degeneration. *Invest. Ophthalmol. Visual Sci.* **2018**, *59*, 4978−4985.

(38) Tachikawa, M.; Takeda, Y.; Tomi, M.; Hosoya, K. Involvement of OCTN2 in the transport of acetyl-L-carnitine across the inner blood-retinal barrier. *Invest. Ophthalmol. Visual Sci.* **2010**, *51*, 430−6.

(39) Pessotto, P.; Valeri, P.; Arrigoni-Martelli, E. The presence of L-carnitine in ocular tissues of the rabbit. *J. Ocul. Pharmacol. Ther.* **1994**, *10*, 643−651.

(40) Alagoz, G.; Celiker, U.; Ilhan, N.; Yekeler, H.; Demir, T.; Celiker, H. L-carnitine in experimental retinal ischemia-reperfusion injury. *Ophthalmologica* **2002**, *216*, 144−150.

(41) Tong, W. H.; Rouault, T. A. Metabolic regulation of citrate and iron by aconitases: role of iron-sulfur cluster biogenesis. *BioMetals* **2007**, *20*, 549−564.

(42) Cheng, Z.; Tsuda, M.; Kishita, Y.; Sato, Y.; Aigaki, T. Impaired energy metabolism in a Drosophila model of mitochondrial aconitase deficiency. *Biochem. Biophys. Res. Commun.* **2013**, *433*, 145−50.

(43) Spiegel, R.; Pines, O.; Ta-Shma, A.; Burak, E.; Shaag, A.; Halvardson, J.; Edvardson, S.; Mahajna, M.; Zenvirt, S.; Saada, A.; Shalev, S.; Feuk, L.; Elpeleg, O. Infantile cerebellar-retinal degeneration associated with a mutation in mitochondrial aconitase, ACO2. *Am. J. Hum. Genet.* **2012**, *90*, 518−23.



https://dx.doi.org/10.1021/acs.jproteome.0c00036
J. Proteome Res. XXXX, XXX, XXX−XXX

(44) Lampropoulou, V.; Sergushichev, A.; Bambouskova, M.; Nair, S.; Vincent, E. E.; Loginicheva, E.; Cervantes-Barragan, L.; Ma, X.; Huang, S. C.; Griss, T.; Weinheimer, C. J.; Khader, S.; Randolph, G. J.; Pearce, E. J.; Jones, R. G.; Diwan, A.; Diamond, M. S.; Artyomov, M. N. Itaconate Links Inhibition of Succinate Dehydrogenase with Macrophage Metabolic Remodeling and Regulation of Inflammation. *Cell Metab.* **2016**, *24*, 158−66.
(45) Kelly, B.; O'Neill, L. A. Metabolic reprogramming in macrophages and dendritic cells in innate immunity. *Cell Res.* **2015**, *25*, 771−84.
(46) Nakamura, R.; Sene, A.; Santeford, A.; Gdoura, A.; Kubota, S.; Zapata, N.; Apte, R. S. IL10-driven STAT3 signalling in senescent macrophages promotes pathological eye angiogenesis. *Nat. Commun.* **2015**, *6*, No. 7847.
(47) Bringmann, A.; Hollborn, M.; Kohen, L.; Wiedemann, P. Intake of dietary salt and drinking water: Implications for the development of age-related macular degeneration. *Mol. Vision* **2016**, *22*, 1437−1454.
(48) Hollborn, M.; Ackmann, C.; Kuhrt, H.; Doktor, F.; Kohen, L.; Wiedemann, P.; Bringmann, A. Osmotic and hypoxic induction of the complement factor C9 in cultured human retinal pigment epithelial cells: Regulation of VEGF and NLRP3 expression. *Mol. Vision* **2018**, *24*, 518−535.
(49) Kim, Y. G.; Lim, H. H.; Lee, S. H.; Shin, M. S.; Kim, C. J.; Yang, H. J. Betaine inhibits vascularization via suppression of Akt in the retinas of streptozotocin-induced hyperglycemic rats. *Mol. Med. Rep.* **2015**, *12*, 1639−1644.
(50) Park, S. W.; Jun, H. O.; Kwon, E.; Yun, J. W.; Kim, J. H.; Park, Y. J.; Kang, B. C.; Kim, J. H. Antiangiogenic effect of betaine on pathologic retinal neovascularization via suppression of reactive oxygen species mediated vascular endothelial growth factor signaling. *Vasc. Pharmacol.* **2017**, *90*, 19−26.
(51) Kersten, E.; Dammeier, S.; Ajana, S.; Groenewoud, J. M. M.; Codrea, M.; Klose, F.; Lechanteur, Y. T.; Fauser, S.; Ueffing, M.; Delcourt, C.; Hoyng, C. B.; de Jong, E. K.; den Hollander, A. I.; Consortium, E.-R. Metabolomics in serum of patients with non-advanced age-related macular degeneration reveals aberrations in the glutamine pathway. *PLoS One* **2019**, *14*, No. e0218457.
(52) Liu, P.; Thomson, B. R.; Khalatyan, N.; Feng, L.; Liu, X.; Savas, J. N.; Quaggin, S. E.; Jin, J. Selective permeability of mouse blood-aqueous barrier as determined by (15)N-heavy isotope tracing and mass spectrometry. *Proc. Natl. Acad. Sci. U.S.A.* **2018**, *115*, 9032−9037.
(53) Cunha-Vaz, J. G. The blood-retinal barriers system. Basic concepts and clinical evaluation. *Exp. Eye Res.* **2004**, *78*, 715−721.
(54) Freddo, T. F. A contemporary concept of the blood-aqueous barrier. *Prog. Retinal Eye Res.* **2013**, *32*, 181−95.
(55) Riley, M. V. Intraocular dynamics of lactic acid in the rabbit. *Invest. Ophthalmol.* **1972**, *11*, 600−607.
(56) Lenth, R. V. Some Practical Guidelines for Effective Sample Size Determination. *Am. Stat.* **2001**, *55*, 187−193.
(57) Laíns, I.; Gantner, M.; Murinello, S.; Lasky-Su, J. A.; Miller, J. W.; Friedlander, M.; Husain, D. Metabolomics in the study of retinal health and disease. *Prog. Retinal Eye Res.* **2019**, *69*, 57−79.


https://dx.doi.org/10.1021/acs.jproteome.0c00036
*J. Proteome Res.* XXXX, XXX, XXX−XXX